

A Wavelet Approach to Finding Steady-State Power Electronics Waveforms Using Discrete Convolution

Kam C. Tam, Siu Chung Wong and Chi K. Tse

Department of Electronic and Information Engineering, Hong Kong Polytechnic University, Hong Kong
http://chaos.eie.polyu.edu.hk

Abstract— Due to the switching action and the presence of parasitics, waveforms arising from power electronics circuits often contain high-frequency ringings embedded in slowly varying segments. Such a feature is consistent with the localization property of wavelets which has been exploited for fast approximations of steady-state waveforms. This paper proposes an improved and more robust approach for calculating the wavelet coefficients, exploiting the orthogonality property of the Chebyshev polynomials.

1. Introduction

Some preliminary work on the analysis of power electronics waveforms using wavelets was reported by Wernke-inck, Valenzuela and Anfossi [1]. Recently, a systematic algorithm for approximating steady-state waveforms arising from power electronics circuits using wavelets has been reported by Tse and co-workers [2, 3]. The advantages of using wavelets for the analysis of power electronics circuits have also been demonstrated. The original algorithm employs a standard curve-fitting method, which uses the boundary conditions together with extra interpolation points for solving the wavelet coefficients. The accuracy of the approximated solution is therefore dependent upon the position of the interpolation points and limited by the wavelet levels used. It has been found that the solution is very sensitive to the choice of interpolation points for obtaining wavelets coefficients, reducing the robustness of the method. The aim of this paper is to tackle the limitations in the standard curve-fitting method. We will provide a new technique for obtaining better approximated waveforms with the same number of wavelet levels.

2. Review of Orthogonality in Chebyshev Polynomials

One important property of Chebyshev polynomials is that they are orthogonal in the sense that their inner product [4, 5, 6], defined by

$$\langle T_m, T_n \rangle \stackrel{\text{def}}{=} \int_{-1}^{+1} \frac{T_m(x)T_n(x)}{\sqrt{1-x^2}} dx, \quad (1)$$

has the following property:

$$\langle T_m, T_n \rangle = \begin{cases} 0 & \text{if } m \neq n \\ \pi & \text{if } m = n = 0 \\ \pi/2 & \text{if } m = n \neq 0. \end{cases} \quad (2)$$

It is always possible to convert a (continuous) orthogonality relationship, as defined in (1), into a discrete orthogonality relationship simply by replacing the integral with a summation. In general, of course, the result is only approximately true. However, where trigonometric functions or Chebyshev polynomials are involved, there are many cases in which the discrete orthogonality can be shown to hold exactly, e.g.,

$$\langle T_m, T_n \rangle \stackrel{\text{def}}{=} \sum_{k=1}^{i+1} T_m(x_k)T_n(x_k) \quad \text{for } 0 \leq m, n \leq i \quad (3)$$

where x_k are the zeros of $T_{i+1}(x)$. Here, we have

$$x_k = \cos \theta_k, \theta_k = \frac{(k - \frac{1}{2})\pi}{i + 1} \quad (4)$$

satisfying the orthogonality condition, i.e.,

$$\langle T_m, T_n \rangle = \begin{cases} 0 & \text{if } m \neq n; m, n \leq i \\ (i + 1) & \text{if } m = n = 0; m \leq i \\ (i + 1)/2 & \text{if } m = n \neq 0; m \leq i. \end{cases} \quad (5)$$

3. Wavelet Approximation of Power Electronics Waveforms Using Discrete Convolution

It has been shown [2] that wavelet approximation can be useful for approximating steady-state solutions of nonlinear circuits without solving systems of nonlinear equations. In most cases, power electronics circuits can be represented by a time-varying state-space equation

$$\dot{\mathbf{x}} = \mathbf{A}\mathbf{x} + \mathbf{U}(t) \quad (6)$$

where \mathbf{x} is the m -dim state vector, \mathbf{A} is an $m \times m$ time-varying matrix, and \mathbf{U} is the input function. Specifically we write

$$\mathbf{A}(t) = \begin{bmatrix} a_{11}(t) & a_{12}(t) & \cdots & a_{1m}(t) \\ \vdots & \vdots & \ddots & \vdots \\ a_{m1}(t) & a_{m2}(t) & \cdots & a_{mm}(t) \end{bmatrix} \quad (7)$$

and

$$\mathbf{U}(t) = \begin{bmatrix} u_1(t) \\ \vdots \\ u_m(t) \end{bmatrix}. \quad (8)$$

In the steady state, the solution satisfies

$$x(t) = x(t + T) \text{ for } 0 \leq t \leq T \quad (9)$$

where T is the period. For an appropriate translation and scaling, the boundary condition can be mapped to the closed interval $[-1, 1]$

$$x(+1) = x(-1) \quad (10)$$

Assume that the basic time-invariant approximation equation is

$$x_i(t) = \mathbf{K}_i^T \Psi(t), \text{ for } -1 \leq t \leq 1 \text{ and } i = 1, 2, \dots, m \quad (11)$$

where $\Psi(t)$ is any wavelet basis of size $2^{n+1} + 1$ (n being the wavelet level) constructed from Chebyshev polynomials,¹ $\mathbf{K}_i^T = [k_{i,0} \ \dots \ k_{i,2^{n+1}}]$ is a coefficient vector of dimension $2^{n+1} + 1$, which has to be found.

The wavelet transformed equation of (6) is

$$\mathbf{K} \mathbf{D} \Psi = \mathbf{A}(t) \mathbf{K} \Psi + \mathbf{U}(t) \quad (12)$$

where

$$\mathbf{K} = \begin{bmatrix} k_{1,0} & k_{1,1} & \dots & k_{1,2^{n+1}} \\ k_{2,0} & k_{2,1} & \dots & k_{2,2^{n+1}} \\ \vdots & \vdots & \ddots & \vdots \\ k_{m,0} & k_{m,1} & \dots & k_{m,2^{n+1}} \end{bmatrix}. \quad (13)$$

Thus, (12) can be written generally as

$$\mathbf{F}(t) \bar{\mathbf{K}} = -\mathbf{U}(t) \quad (14)$$

where $\mathbf{F}(t)$ is a $m \times (2^{n+1} + 1)m$ matrix, as given by

$\mathbf{F}(t) =$

$$\begin{bmatrix} a_{11}(t) \Psi^T(t) \mathbf{D}^T & & & & \\ & -\Psi^T(t) \dots & a_{1i}(t) \Psi^T(t) & \dots & a_{1m} \Psi^T(t) \\ & \vdots \ddots & \vdots & \ddots & \vdots \\ a_{i1}(t) \Psi^T(t) \dots & & a_{ii}(t) \Psi^T(t) & \dots & a_{im} \Psi^T(t) \\ & & & -\Psi^T(t) \mathbf{D}^T & \\ & \vdots \ddots & \vdots & \ddots & \vdots \\ a_{m1}(t) \Psi^T(t) \dots & & a_{mi}(t) \Psi^T(t) & \dots & a_{mm} \Psi^T(t) \\ & & & & -\Psi^T(t) \mathbf{D}^T \end{bmatrix}$$

and $\bar{\mathbf{K}}$ is a $(2^{n+1} + 1)m$ -dim vector given by

$$\bar{\mathbf{K}} = [\mathbf{K}_1^T \ \dots \ \mathbf{K}_m^T]^T. \quad (15)$$

Note that since the unknown $\bar{\mathbf{K}}$ is of dimension $(2^{n+1} + 1)m$, we need $(2^{n+1} + 1)m$ equations. Now, the boundary condition (10) provides m equations, i.e.,

$$[\Psi(1) - \Psi(-1)]^T \mathbf{K}_i = \mathbf{0}, \text{ for } i = 1, \dots, m. \quad (16)$$

¹The construction of wavelet basis has been discussed in detail in Liu *et al.* [2] and more formally in Frazier [7].

In the original curve-fitting approach, $2^{n+1}m$ equations are obtained by interpolating at 2^{n+1} distinct points in the closed interval $[-1, 1]$, and the interpolation points are chosen from the zeros of Chebyshev polynomials of the second kind, i.e.,

$$\eta_i^{(2^{n+1})} = \cos\left(\frac{i\pi}{2^{n+1}}\right). \quad (17)$$

It is obvious from (16) that one of the end points of either $\eta_0 = 1$ or $\eta_{2^{n+1}} = -1$ must be excluded from the interpolation points, as will be discussed in Section 4. In contrast, our new approach here takes advantage of the orthogonality in Chebyshev polynomials. The $2^{n+1}m$ more equations are obtained by taking discrete convolution over the closed interval $[-1, 1]$ with T_i for $i = 0, \dots, 2^{n+1} - 1$. The number of points for discrete convolution is therefore no longer limited by the wavelet level in the calculation. Thus, this discrete convolution approach gives a more robust and more accurate solution. In discrete convolution, the approximation equation can be written as

$$\tilde{\mathbf{F}} \bar{\mathbf{K}} = \tilde{\mathbf{U}} \quad (18)$$

where

$$\tilde{\mathbf{F}} = \begin{bmatrix} \tilde{\mathbf{F}}_1 \\ \tilde{\mathbf{F}}_2 \end{bmatrix} \text{ and } \tilde{\mathbf{U}} = \begin{bmatrix} \tilde{\mathbf{U}}_1 \\ \tilde{\mathbf{U}}_2 \end{bmatrix} \quad (19)$$

and $\tilde{\mathbf{F}}_1$, $\tilde{\mathbf{F}}_2$, $\tilde{\mathbf{U}}_1$ and $\tilde{\mathbf{U}}_2$ are given by

$$\tilde{\mathbf{F}}_1 = \begin{bmatrix} [\Psi(1) & (0 \ 0 \ \dots \ 0) & \dots & (0 \ 0 \ \dots \ 0) \\ -\Psi(-1)]^T & [\Psi(1) & \dots & (0 \ 0 \ \dots \ 0) \\ (0 \ 0 \ \dots \ 0) & -\Psi(-1)]^T & & \\ \vdots & \vdots & \ddots & \vdots \\ & & & [\Psi(1) \\ (0 \ 0 \ \dots \ 0) & (0 \ 0 \ \dots \ 0) & \dots & -\Psi(-1)]^T \\ \underbrace{\hspace{10em}}_{2^{n+1} + 1 \text{ columns}} & & & \\ \underbrace{\hspace{10em}}_{(2^{n+1} + 1)m \text{ columns and } m \text{ rows}} \end{bmatrix}$$

$$\tilde{\mathbf{F}}_2 = \left. \begin{bmatrix} \langle \mathbf{F}(t), T_0(t) \rangle \\ \langle \mathbf{F}(t), T_1(t) \rangle \\ \vdots \\ \langle \mathbf{F}(t), T_{2^{n+1}-1}(t) \rangle \end{bmatrix} \right\} 2^{n+1}m \text{ rows}$$

$$\tilde{\mathbf{U}}_1 = \left. \begin{bmatrix} 0 \\ \vdots \\ 0 \end{bmatrix} \right\} m \text{ elements}$$

$$\tilde{\mathbf{U}}_2 = \left. \begin{bmatrix} \langle -\mathbf{U}(t), T_0(t) \rangle \\ \langle -\mathbf{U}(t), T_1(t) \rangle \\ \vdots \\ \langle -\mathbf{U}(t), T_{2^{n+1}-1}(t) \rangle \end{bmatrix} \right\} 2^{n+1}m \text{ elements}$$

with $\langle \mathbf{F}(t), T_k(t) \rangle$ representing a new matrix whose elements are the corresponding convolutions with T_k . By

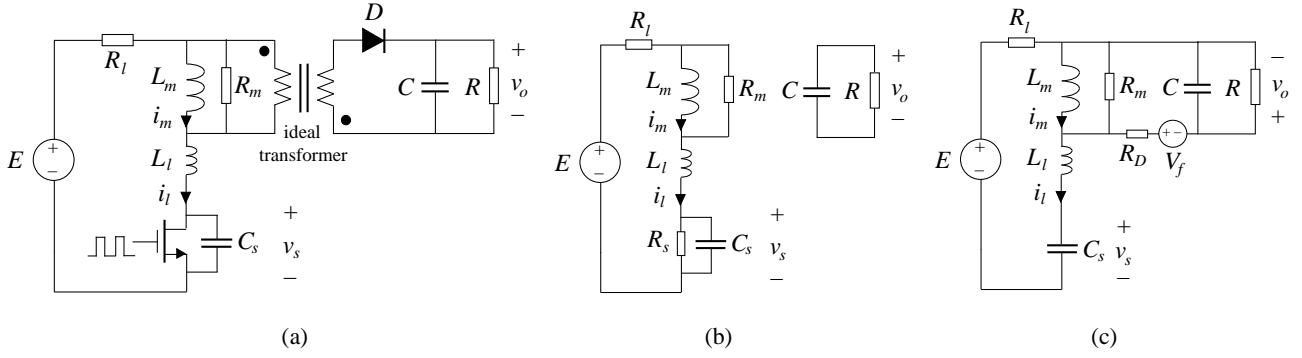


Figure 1: (a) Flyback converter model with transformer leakage inductance and switching device parasitic capacitance; (b) on-time circuit model; (c) off-time circuit model.

solving (18), we obtain all the coefficients necessary for generating an approximate solution for the steady-state system.

4. Simulations and Evaluations

The results are evaluated using the *mean relative error* (MRE) and *mean absolute error* (MAE), which are defined as

$$\text{MRE} = \frac{1}{N} \sum_{i=1}^N \left| \frac{\hat{x}_i - x_i}{x_i} \right| \quad (20)$$

$$\text{MAE} = \frac{1}{N} \sum_{i=1}^N |\hat{x}_i - x_i| \quad (21)$$

where N is the total number of points sampled along the interval $[-1, 1]$ for error calculation. In the following, we use uniform sampling (i.e., equal spacing) with $N = 1001$, including boundary points.

Example: Flyback Converter with Parasitic Ringings

We consider the flyback converter shown in Fig. 1 (a). This is a more realistic model as the parasitic capacitance across the switch and leakage inductance of the transformer are deliberately included. The operation is as follows. When the switch is turned on, current flows through the magnetizing inductance L_m and the leakage inductance L_l , with the transformer secondary opened and the diode not conducting. When the switch is turned off, the transformer secondary conducts through the diode, clamping the primary voltage (i.e., voltage across L_m) to the output network (assuming a 1:1 turns ratio). Thus, L_m discharges through the transformer primary, while the leakage L_l and the parasitic capacitance C_s form a damped resonant loop around the input voltage source. Figs. 1 (b) and (c) show the detailed circuit models for the on-time and off-time durations, respectively.

The state equation of this converter is given by

$$\dot{\mathbf{x}} = \mathbf{A}(t)\mathbf{x} + \mathbf{U}(t) \quad (22)$$

Table 1: Component and Parameter Values for Simulation.

Component/Parameter	Value
Magnetizing (storage) inductance, L_m	0.4 mH
Leakage inductance, L_l	1 μ H
Equivalent parallel resistance of transformer primary, R_m	1 M Ω
Output capacitance, C	0.1 mF
Load resistance, R	12.5 Ω
Input voltage, E	16 V
Diode forward drop, V_f	0.8 V
Switching period, T	100 μ s
On-time, T_D	45 μ s
Equivalent loop resistance, R_l	0.4 Ω
Switch on-resistance, R_S	0.001 Ω
Switch capacitance, C_S	200 nF
Diode on-resistance, R_D	0.001 Ω

where $\mathbf{x} = [i_m \ i_l \ v_s \ v_o]^T$, and $\mathbf{A}(t)$ and $\mathbf{U}(t)$ are given by

$$\mathbf{A}(t) = \mathbf{A}_1(1 - s(t)) + \mathbf{A}_2s(t) \quad (23)$$

$$\mathbf{U}(t) = \mathbf{U}_1(1 - s(t)) + \mathbf{U}_2s(t) \quad (24)$$

with $s(t)$ defined as

$$s(t) = \begin{cases} 0 & \text{for } 0 \leq t \leq T_D \\ 1 & \text{for } T_D \leq t \leq T \\ s(t - T) & \text{for all } t > T. \end{cases} \quad (25)$$

and the \mathbf{U} 's and \mathbf{A} 's being derivable from the circuit topologies.

The parameters for simulation are listed in Table 1. We have compared the approximated waveforms of the leakage inductor current for both discrete convolution and curve-fitting method. Figs. 2 (a) and (b) show the approximated waveforms using discrete convolution at two different wavelet levels. Figs. 2 (c) and (d) show the approximated waveforms using the curve-fitting approach, excluding $\eta_{2n+1} (= -1)$ and $\eta_0 (= 1)$ respectively. As there is no systematic method to predict which exclusion would produce better result, the original curve-fitting method is less robust.

Table 2: Comparison of MAEs. All Wavelets up to levels 5, 6, 7 and 8 are Used for Approximating the Leakage Inductor Current in Flyback Converter.

Wavelet levels	Number of wavelets	MAE for i_l (curve fitting)	MAE for i_l (proposed)
-1 to 5	65	0.60376	0.24045
-1 to 6	129	0.52070	0.15298
-1 to 7	257	0.36704	0.15314
-1 to 8	513	0.18808	0.16106

Since the waveform contains a substantial portion where the value is near zero, we use the MAE as the evaluation metric. Better results from the original method are selected for comparison in Table 2 which clearly verifies the advantage of using discrete convolution for wavelet approximation.

5. Conclusion

In this paper, we propose a robust algorithm for approximating waveforms of power electronics using wavelets. The algorithm exploits the orthogonality property to provide the necessary alternative equations for solving the wavelet coefficients. Furthermore, it has been shown that the discrete convolution method offers good robustness as well as numerical accuracy over the original curve-fitting approach. Moreover, further work should be directed in choosing an appropriate wavelet basis for an analytical convolution for further reducing computational cost. With analytical convolution, the algorithm can be designed to contain pre-calculated analytical solutions, allowing the unknown wavelet coefficients to be found very quickly. This will be reported in a future publication.

Acknowledgement

This work was supported by a research grant provided by the Hong Kong Polytechnic University (Project A-PD68).

References

- [1] E. Wernekinck, H. Valenzuela, and I. Anfossi, "On the analysis of power electronics circuits waveforms with wavelets," *Proc. Power Conversion Conf.*, pp. 544–549, 1993.
- [2] M. Liu, C.K. Tse, and J. Wu, "A wavelet approach to fast approximation of steady-state waveforms of power electronics circuits," *Int. J. Circuit Theory Appl.*, vol. 31, no. 6, pp. 591–610, November 2003.
- [3] M. Liu, P.W.M. Ho, C.K. Tse and J. Wu, "Application of wavelet transform to steady-state approximation of power electronics waveforms," *Proc. IEEE Int. Symp. Circuits and Systems (ISCAS'03)*, pp. 336–339, May 2003.
- [4] J. C. Mason and D. C. Handscomb, *Chebyshev Polynomials*, Boca Raton: Chapman and Hall/CRC, 2003.
- [5] T. Kilgore and J. Prestin, "Polynomial wavelets on the interval," *Constructive Approximation*, vol. 12, pp. 95–110, 1995.
- [6] B. Fisher and J. Prestin, "Wavelets based on orthogonal polynomials," *Math. of Computation*, vol. 66, no. 220, pp. 1593–1618, 1997.
- [7] M. W. Frazier, *An Introduction to Wavelets Through Linear Algebra*, New York: Springer-Verlag, 1999.

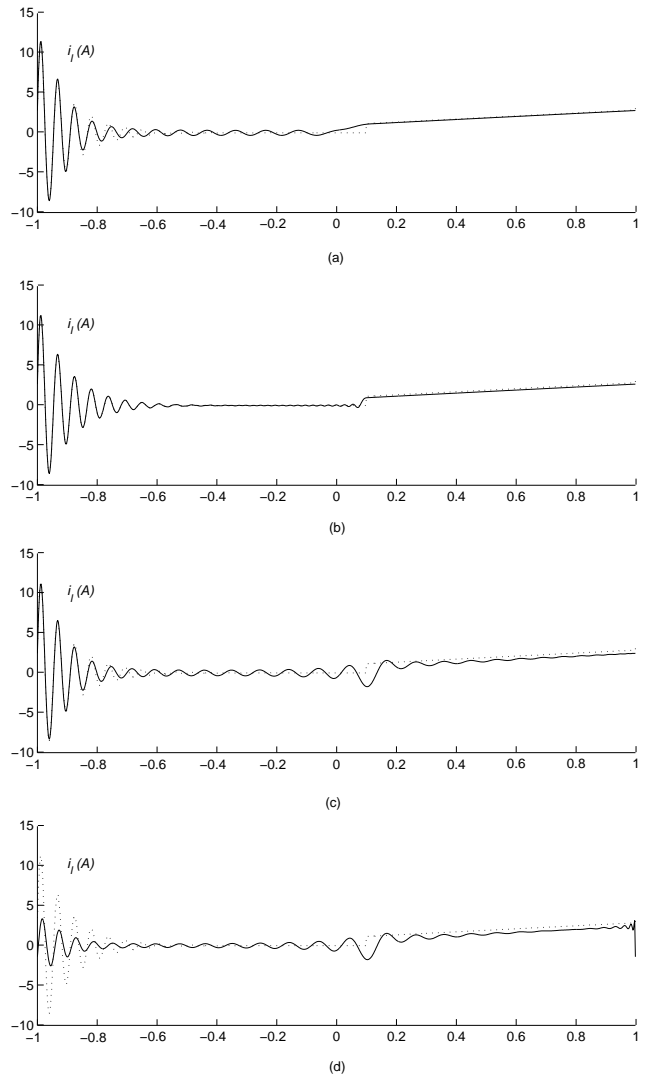


Figure 2: Inductor waveforms of flyback converter. Dashed line is waveform from SPICE simulation. Solid line is approximated waveform. (a) Using discrete convolution wavelets of level -1 to 5; (b) using discrete convolution wavelets of level -1 to 7; (c) using curve-fitting wavelets of level -1 to 5 excluding the interpolation point $\eta_{2^{n+1}} (= -1)$; and (d) using curve-fitting wavelets of level -1 to 5 excluding the interpolation point $\eta_0 (= 1)$.